Organic & Biomolecular Chemistry

Cite this: *Org. Biomol. Chem.*, 2011, **9**, 1061

www.rsc.org/obc

PAPER

Inclusion complex formation of sanguinarine alkaloid with cucurbit[7]uril: inhibition of nucleophilic attack and photooxidation†

Zsombor Miskolczy, Mónika Megyesi, Gábor Tárkányi, Réka Mizsei and László Biczók*

Received 4th September 2010, Accepted 2nd November 2010
DOI: 10.1039/c0ob00666a

The inclusion of sanguinarine, a biologically active natural benzophenanthridine alkaloid, in cucurbit[7]uril (CB7) was studied by NMR and ground-state absorption spectroscopy, as well as steady-state and time-resolved fluorescence measurements in aqueous solution. The iminium form of sanguinarine (SA^+) produces very stable 1 : 1 inclusion complex with CB7 ($K = 1.0 \times 10^6$ M^{-1}), whereas the equilibrium constant for the binding of the second CB7 is about 3 orders of magnitude smaller. Marked fluorescence quantum yield and fluorescence lifetime enhancements are found upon encapsulation of SA^+ due to the deceleration of the radiationless deactivation from the single-excited state, but the fluorescent properties of 1 : 1 and 1 : 2 complexes barely differ. The equilibrium between the iminium and alkanolamine forms is shifted 3.69 pK unit upon addition of CB7 as a consequence of the preferential encapsulation of the iminium form and the protection of the 6 position of sanguinarine against the nucleophilic attack by hydroxide anion. On the basis of thermodynamic cycle, about 225 M^{-1} is estimated for the equilibrium constant of the complexation between the alkanolamine form of sanguinarine (SAOH) and CB7. The confinement in the CB7 macrocycle can be used to impede the nucleophilic addition of OH^- to SA^+ and to hinder the photooxidation of SAOH.

Introduction

Encapsulation of species of biological interest in macrocyclic compounds have been extensively studied because it can be utilized in the delivery, stabilization, solubilization and controlled release of drugs as well as in analyte sensing. Cyclodextrins are the most widely used hosts in these applications.[1] Recent reviews provide good overview on the biopharmacological utilizations of water-soluble calixarenes.[2,3] Cucurbit[*n*]urils (CBn), the family of relatively new, pumpkin-shaped cavitands composed of *n* glycoluril units,[4] are able to cross the cell membrane, which can be exploited for drug delivery.[5] The interaction of the lactone and carboxylate forms of camptothecin, a cytotoxic quinoline alkaloid, with CBn was examined and the effect of inclusion complex formation on the solubility and anticancer activity was revealed.[6] A significant increase of thermal stability upon encapsulation in cucurbit[7]uril (CB7) was found for ranitidine, a histamine H_2-receptor antagonist employed for the treatment of excess stomach acid production.[7] The stability constants for the inclusion of local anaesthetics in CB7 are 2–3 orders of magnitude greater than the values reported for binding by the comparably sized β-cyclodextrin host molecule.[8] CBn complexation may provide a formulation method to solubilize albendazole, an anticancer agent,[9] and its derivatives[10] for clinical application. Nau's group have shown that the embedment of the benzimidazole moiety of the proton-pump inhibitor lansoprazole and omeprazole drugs not only catalyzes the transition into their physiologically active cyclic sulfenamide form but also hinders the decomposition and dimerization, while the biologically important reactivity is retained.[11] The embedment of antitumor platinum(II) complexes in CBn provides steric hindrance to drug degradation by peptides and proteins, and the use of different sized macrocycles allows of the tuning of drug release rates and toxicity.[12] Antitumor metallocenes also form inclusion complex with CBn. The molibdocene complex catalysed the degradation of the cucurbituril framework in the presence of oxygen, whereas encapsulation of titanocene dichloride by CB7 greatly slowed the hydrolysis of the cyclopentadienyl ligands.[13] For targeted drug delivery, stimuli-responsive polymer nanocapsules,[14] and reduction-sensitive, biocompatible vesicles were self-assembled using cucurbit[6]uril (CB6) macrocycles.[15] Noninvasive remote-controlled release of drug molecules was achieved from magnetic-core silica nanoparticles capped with CB6.[16]

Despite the pharmaceutical importance of natural alkaloids very few information is available on their complexation with CBn. The basicity of a pyridoindole type alkaloid, norharmane increased only 0.7 pK unit upon inclusion.[17] The isoquinoline alkaloid, berberine proved to be a very sensitive fluorescent probe,[18] and 500-fold fluorescence quantum yield enhancement was observed upon binding in CB7.[19] Sensitive analytical methods have been developed on the basis of CBn complex formation for the quantitative determination of coptisine[20] and sanguinarine[21] in biological fluids.

Chemical Research Center, Hungarian Academy of Sciences, P.O. Box 17, 1525, Budapest, Hungary. E-mail: biczok@chemres.hu; Fax: +36-1-438-1143

† Electronic supplementary information (ESI) available. See DOI: 10.1039/c0ob00666a

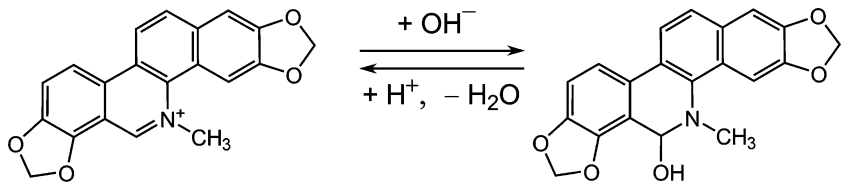

Scheme 1 The two forms of sanguinarine.

Several studies have dealt with the effect of encapsulation in CBn on the protonation of guests,[7,11,22] but it is unknown how the encapsulation influences the nucleophilic attack of organic compounds. In the present work, we focus on sanguinarine, a natural benzo[c]phenanthridine alkaloid (Scheme 1), which exhibits anticancer, antimicrobial, antifungal properties[23] and interacts with nucleic acids.[24] A pH dependent reversible transition occurs between its iminium (SA^+) and alkanolamine (SAOH) forms.[25,26] Since the carbon atom of SA^+ at the position 6 has low π-electron density,[27] it is susceptible to nucleophilic addition of OH^-. The biological activity is associated with the SA^+ form, whereas the conversion to SAOH enhances the lipophilicity improving thereby the cellular availability.[26] The latter form undergoes an irreversible oxidation in the singlet-excited state to produce oxysanguinarine.[28] The main goal of the present studies was to reveal how the interaction with CB7 affects the fluorescent properties, photostability and the basicity of sanguinarine. Moreover, we demonstrate that SA^+ can associate with not only one but also two CB7 macrocycle.

Results and discussion

Inclusion complex formation studied by NMR spectroscopy

Systematic NMR studies provide valuable information on the structure and stoichiometry of inclusion complex formation. Because of the inherently lower sensitivity of this technique, much more concentrated sanguinarine solutions (typically 0.4–1 mM) had to be used than in absorption and fluorescence spectroscopic measurements. The high frequency region of the ^{1}H-NMR spectrum (6.0–10.0 ppm) proved to be appropriate to monitor the chemical shift changes of SA^+. Spectral assignment of the SA^+ protons was performed in the absence of CB7 by ^{1}H-^{13}C long-range *J*-correlation (gHMBC) and spatial correlation (1D-ROESY) experiments. For the complexes, homonuclear ^{1}H-^{1}H NOESY and ^{1}H-^{1}H ROESY spectra were recorded.

Fig. 1 displays the effect of complexation on the spectrum of SA^+ at 283 K. The upper panel presents the spectrum of free SA^+ in neat D_2O, whereas the lower panel shows the spectral alterations upon the gradual increase of SA^+ concentration in 1 mM CB7 solution. The signal of H-6 is identified in all spectra indicating that the iminium form (SA^+) dominates over the SAOH form under the condition of the NMR measurements (pH ≈ 6). At 0.1–0.2 mM SA^+ concentration range a single set of resonances appears, where most aromatic protons have significant chemical shift displacements with respect to the uncomplexed SA^+. This spectrum is assigned to 1 : 2 SA^+:CB7 inclusion complex. The methylenes I and II of this species experience a significant shielding effect due to the encapsulation in CB7 cavity and their resonances are shifted upfield into the 4–5 ppm region of the ^{1}H-NMR spectrum overlapping with the solvent and CB7 signals. Therefore, the resonances of I and II are missing from the spectra. Substantial upfield displacements are also observed for H-1 and H-9 resonances upon complexation, which is in line with the fact that both ends of SA^+ are embedded in a different CB7 macrocycle. Scheme 2 illustrates the processes taking place in the solution containing SA^+ and CB7.

At 0.3 mM SA^+ concentration, a second set of resonances emerges due to the partial dissociation of the 1 : 2 complex into 1 : 1 associate. In the spectrum of the latter species, the methylene I peak moves to upfield into the domain of the solvent and CB7 signals, which is accompanied by the significant upfield displacement of the signal of H-9 and H-10. The geminal protons of the methylene II show chemical non-equivalence possibly due to the induced diastereotopic environment above the rim of the CB7 in the 1 : 1 complex. Therefore, methylene II gives rise to two broadened singlet resonances near ~6.1 ppm having a small (J<2 Hz) two-bond *J*-coupling but the location of the signals barely alters compared to the corresponding resonance for uncomplexed SA^+. These spectral changes suggest that the methylene I end of SA^+ is encapsulated in the 1 : 1 complex.

At large SA^+ concentration, a third set of signals arises parallel with the intensity enhancement of the peaks attributed to the 1 : 1 inclusion complex. Furthermore, the spectrum of the 1 : 2 inclusion complex concomitantly vanishes when the SA^+:CB7 molar ratio grows above 0.5. The third set of signals, coded with orange colour, is probably due to weakly bound species formed by non-specific binding. As shown in Scheme 1, sanguinarine aggregates $(SA^+Cl^-)_n$ and various loosely bound SA^+–CB7 complexes, in which the alkaloid is not inserted into the CB7 cavity, may contribute to the broad resonances coded with orange colour. Fast exchange occurs among these species. In contrast, 1 : 2 and 1 : 1 confinements in CB7 cavity lead to slow exchange among the solutes. Fig. 2 shows the spectral change with increasing temperature. The three sets of ^{1}H-NMR resonances reversibly coalesce into a single broad set, whose chemical shifts differ from those found in the absence of CB7. According to the magnitude of the exchange cross-peaks in the NOESY spectrum (Fig. 3), the extent of the population transfer between the non-specific and 1 : 2 complexes is small, however one can identify intense chemical exchange between non-specific and 1 : 1 complexes and the correlations between 1 : 1 and 1 : 2 inclusion complexes are also well observable in most cases.

Energy-minimized structure of the 1 : 1 and 1 : 2 complexes

To get more information on the molecular structure of SA^+–CB7 complexes, quantum chemical calculations were carried out

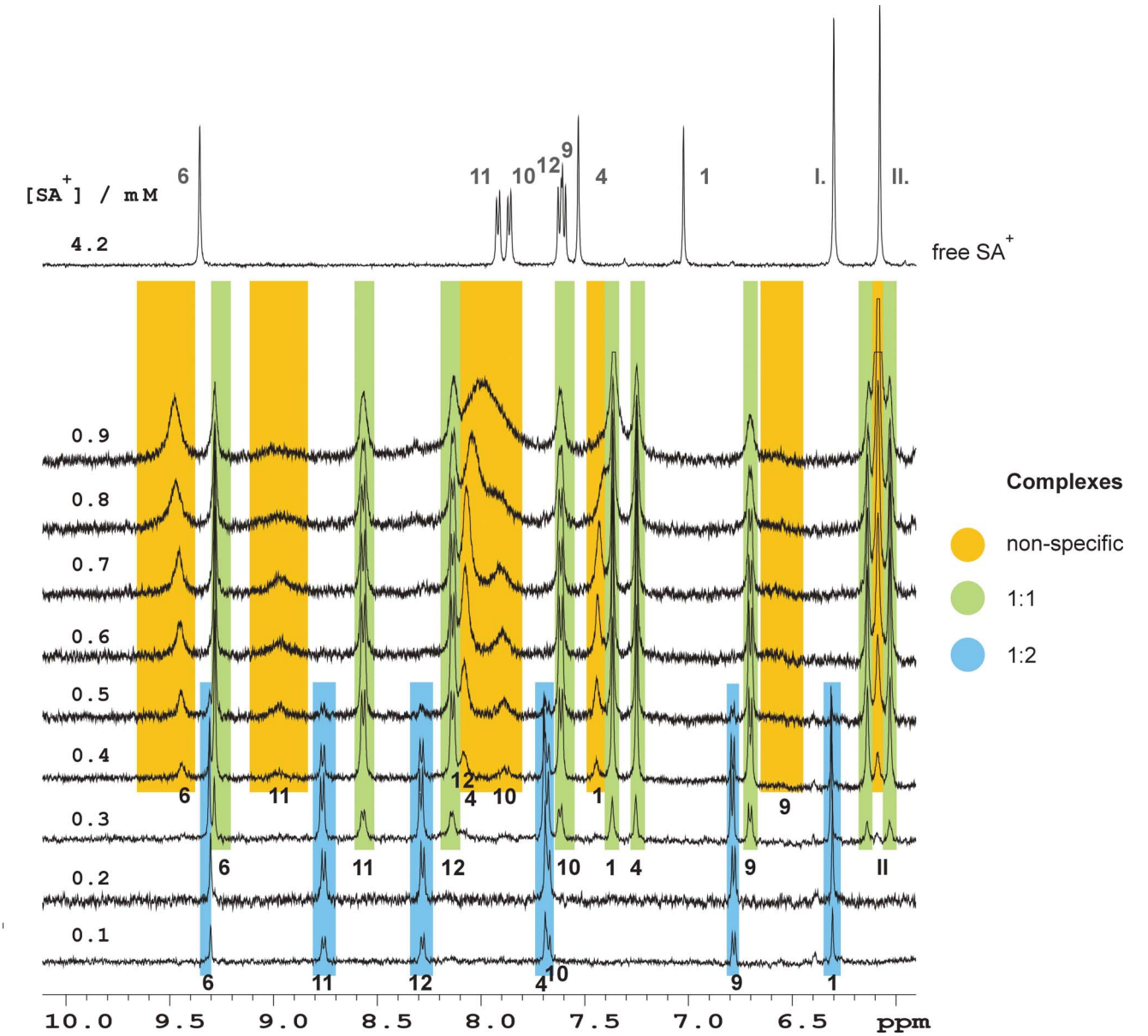

Fig. 1 Aromatic region of the ^{1}H NMR spectra (599.9 MHz, D_2O, 283 K) for SA^+–CB7 mixtures. The amount of CB7 (1.0 mM) was kept constant, while the concentration of SA^+ (indicated on the left) was increased. For comparison, the spectrum of SA^+ recorded in the absence of CB7 is presented on the top. The assignment of the color-coded resonances corresponds to Scheme 2.

with RM1 semiempirical method using HyperChem 8.0 program. The energy-minimized structure of the ground-state complexes are in accordance with the NMR spectra. As shown in the upper panel of Fig. 4, SA^+ can be only partially encapsulated when 1 : 1 complex is formed because the length of CB7[4] is only 0.91 nm. The benzodioxole part of the isoquinoline moiety is encapsulated in the hydrophobic core of CB7 and the positive charge of the nitrogen-heterocyclic ring interacts with the oxygens of the macrocycle. The embedment of the other end of SA^+ is unfavourable because the penetration into the host is hindered sterically by the N-methyl substituent, and the larger distance of the positively charged nitrogen-heterocyclic ring from the carbonyl-laced portal of CB7 does not allow the stabilization of this structure by electrostatic interactions. In addition to these effects, the repulsion between the negatively charged oxygens of the two hosts also renders the binding of two CB7 more difficult. The lower panel of Fig. 4 displays that in the case of the 1 : 2 complex, the positive charge of the nitrogen-heterocyclic ring interacts with both hosts, and the benzodioxole part of the isoquinoline moiety is less deeply incorporated in CB7 than in the 1 : 1 complex. The latter phenomenon may explain the smaller upfield shift of the H-6, H-10 and H-9 resonances for the 1 : 2 complex compared to those observed for the 1 : 1 associate. The quantum chemical calculations show that SA^+ is not planar. Consequently, the CB7 macrocycles do not have a parallel configuration in the 1 : 2 complex.

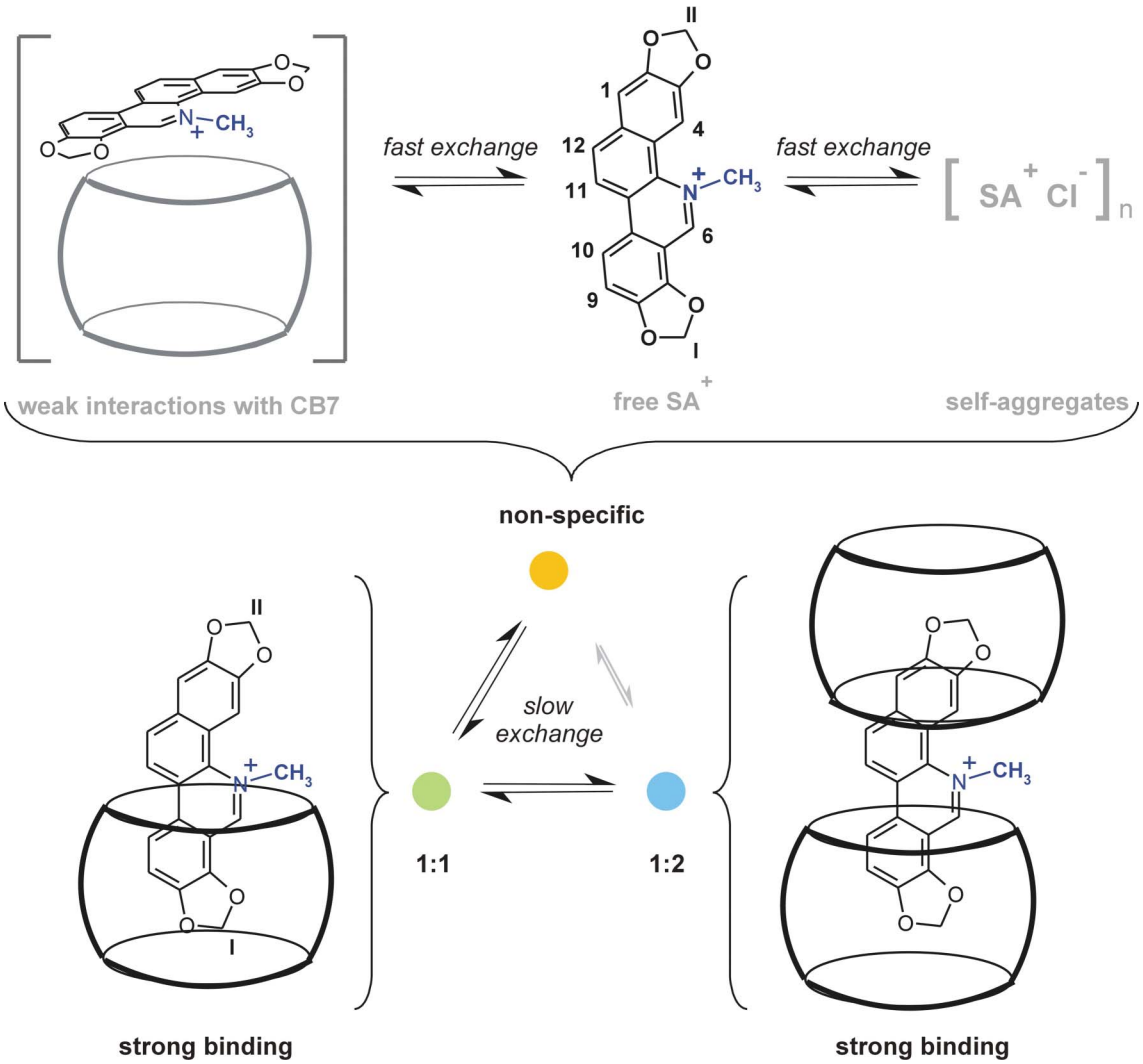

Scheme 2 Binding modes of SA^+ with CB7.

Effect of CB7 on the absorption and fluorescence properties of SA^+ at pH 4

The larger sensitivity of the absorption and fluorescence spectroscopy allowed the study of the complexation with CB7 in much more diluted (16.4 μM) sanguinarine solution, where non-specific binding plays negligible role. To avoid the formation of the alkanolamine form (SAOH), the experiments were performed at pH 4. As seen in Fig. 5, the absorption spectrum exhibits a slight hypsochromic shift on addition of CB7 evidencing complex formation. The inset displays the absorbance change at 490 nm. A marked absorbance diminution is observed in the 0–0.04 mM CB7 concentration range followed by a slight absorbance increase at higher CB7 concentration. The two distinct domains suggest that not only one but also two CB7 can form a complex with a sanguinarine cation, in agreement with the results of NMR studies. The equilibrium constants are defined as

$$K_1 = \frac{[Complex1:1]}{[SA^+][CB7]} \quad (1)$$

$$K_2 = \frac{[Complex1:2]}{[Complex1:1][CB7]} \quad (2)$$

The data of spectrophotometric titration were analyzed by a home-made MATLAB 7.9 program as described in our previous paper.[29] The line in the inset to Fig. 5 corresponds to the optimized parameters: $K_1 = 1.0 \times 10^6$ M^{-1}, $K_2 = 1000$ M^{-1}, ε(Complex1:1) = 3400 $M^{-1}cm^{-1}$ and ε(Complex1:2) = 5000 $M^{-1}cm^{-1}$, where ε(Complex1:1) and ε(Complex1:2) denote the molar absorption coefficients of 1 : 1 and 1 : 2 complexes, respectively.

Binding to CB7 also alters the fluorescent behaviour of SA^+ (Fig. 6). The fluorescence quantum yield of SA^+ grows from 0.038 to 0.37 upon addition of 0.1 mM CB7. When the concentration of CB7 is raised, the emission peak located initially at 604 nm moves gradually to 556 nm, and a concomitant intensity enhancement is observed. As a representative example, the inset shows the fluorescence intensity change at 558 nm and the line represents the result of the nonlinear least-squares analysis. The fitted equilibrium constants are $K_1 = 1.4 \times 10^6$ M^{-1} and

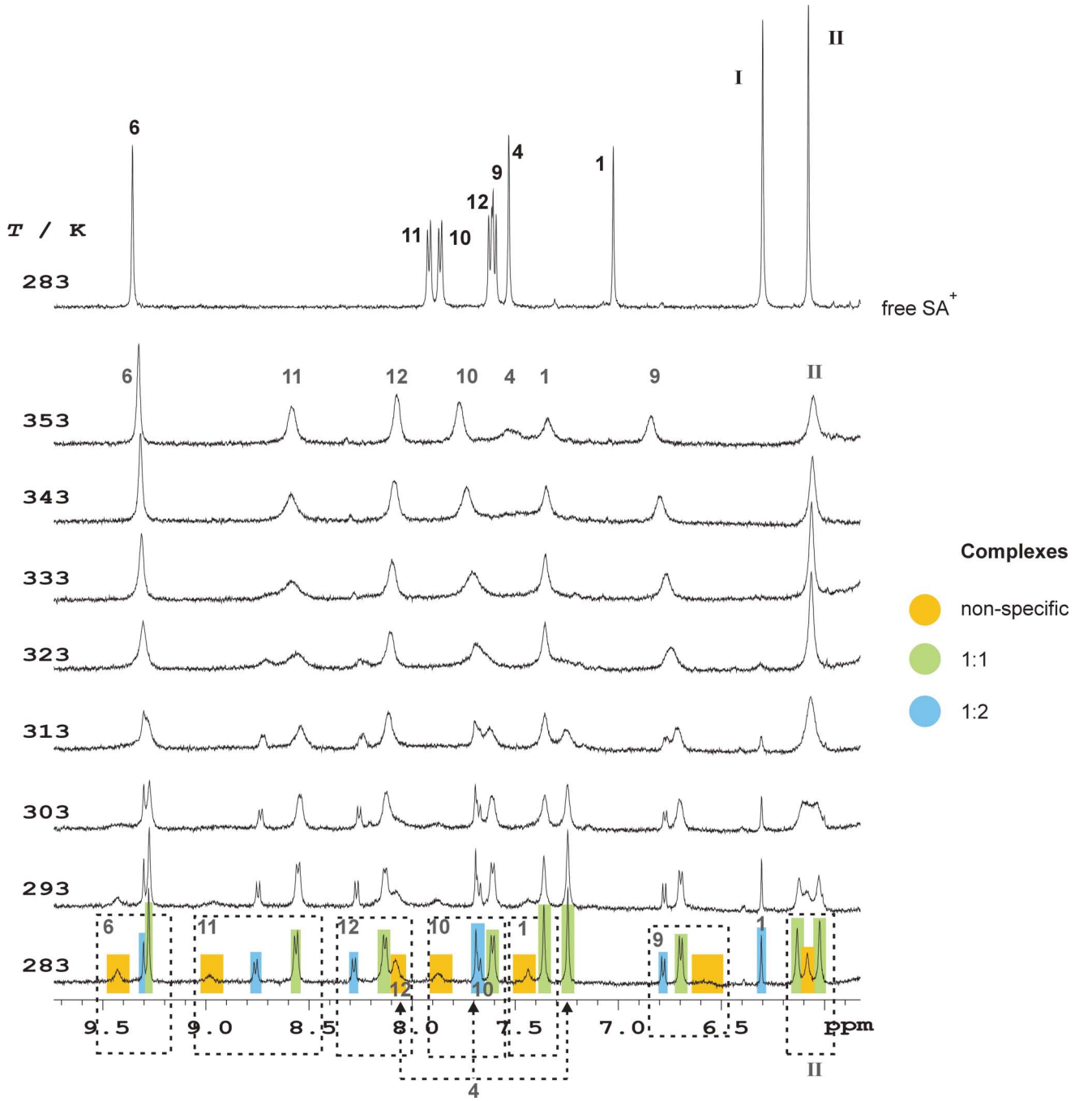

Fig. 2 Aromatic region of the ^{1}H-NMR spectra for 0.43 mM SA^+ and 1 mM CB7 mixture in D_2O (599.9 MHz) as a function of the temperature. The spectrum of free SA^+ (4.2 mM) is shown in the absence of CB7 on the top.

K_2 = 1000 M^{-1}, whereas I_F(Complex1:1)/I_F(SA^+) = 17.7 and I_F(Complex1:2)/I_F(SA^+) = 16.0 are obtained for the fluorescence intensity ratios at the detection wavelength (558 nm).

The fluorescence decay characteristics of SA^+ also change considerably upon 1 : 1 binding to CB7. In accordance with recently published results,[30] exponential fluorescence intensity *vs.* time profiles with τ_1 = 2.3 ns excited-state lifetime is measured in water. Upon gradual addition of CB7, a new fluorescence component with a lifetime of τ_2 = 17.5 ns emerges, whose amplitude grows due to SA^+–CB7 complex formation. Around 13 μM CB7 concentration the amplitude of SA^+ fluorescence vanishes, and only the long-lived fluorescence of SA^+–CB7 1 : 1 complex is detected. Further increase of the amount of CB7 in the solution brings about negligible change in the fluorescence decay indicating that the difference between the fluorescence lifetimes of 1 : 2 and 1 : 1 complexes is less than the limit of experimental errors. The similar enhancement of the apparent fluorescence yield and the fluorescence lifetime implies that the confinement in CB7 affects mainly the rate of nonradiative energy dissipation processes of the singlet-excited SA^+.

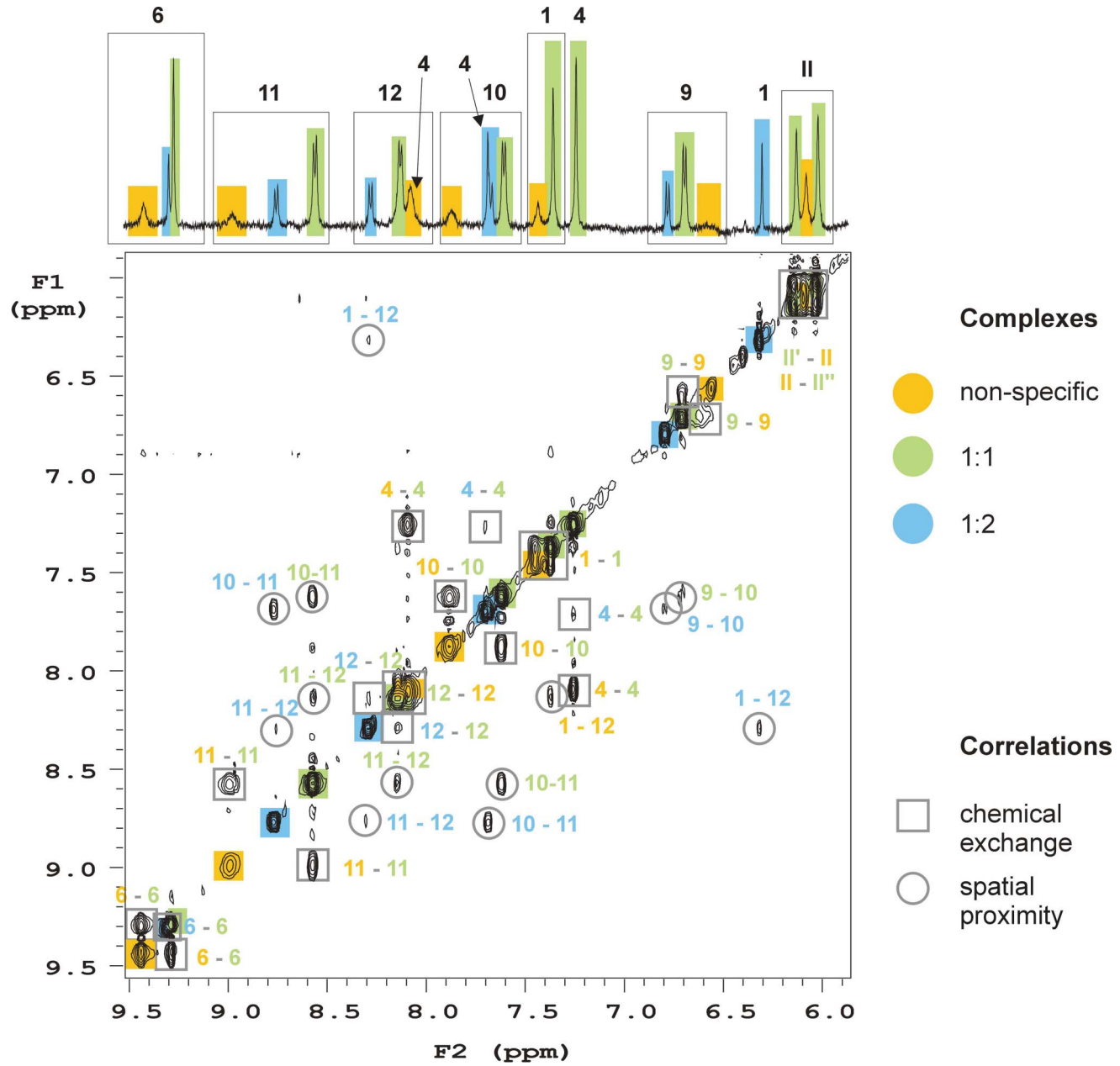

Fig. 3 Aromatic region of the ^{1}H-^{1}H NOESY spectra of 0.43 mM SA^{+} and 1 mM CB7 mixture (599.9 MHz, D_2O, 263 K, $\tau_{mix} = 0.1$ s). The cross-peaks stem from two types of correlations. The intense ones are exchange cross-peaks which appear between the same protons of SA^{+} that correspond to the different binding states (□). There are also NOE type cross-peaks encoding the spatial proximity between neighboring protons of the same species (○).

Effect of pH variation

As Absolínová and co-workers pointed out,[25c] there is a considerable discrepancy in the literature among the pK values measured by various experimental techniques for the pH dependent equilibrium between the iminium (SA^{+}) and alkanolamine (SAOH) forms of sanguinarine. The ionic strength, buffer, added organic solvent, interaction with anions and the low solubility of SAOH modify the pK values. To avoid these effects, acid–base titration was performed in dilute neat aqueous solution. The results of the absorption and fluorescence spectroscopic studies carried out in the absence and presence of CB7 are compared in Fig. 7B. The pH dependence of the sanguinarine spectra in CB7 solution (Fig. 7A) is qualitatively similar to that found in water, but the alterations appear at much higher pH. Increasing OH^{-} concentration leads to the gradual disappearance of the SA^{+} absorption in the 380–520 nm range and the fluorescence band in the 470–740 nm domain because the nucleophilic addition to the carbon atom of the iminium bond eliminates the aromaticity of the heterocyclic ring. The SAOH form absorbs only UV light, and its fluorescence band is strongly blue-shifted compared to that of SA^{+}. The fluorescence maximum of SAOH is located at 415 nm in water, whereas it is red-shifted to 419 nm in 1 mM CB7 solution indicating that SAOH is able to produce inclusion complex with CB7.

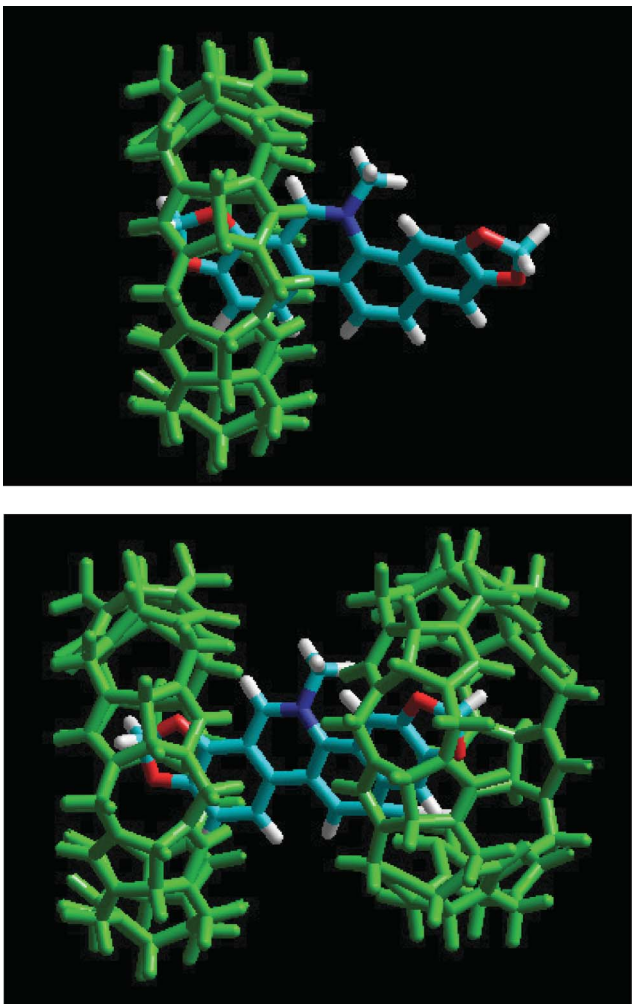

Fig. 4 Energy-minimized structure of the 1 : 1 and 1 : 2 SA^+–CB7 complexes in the ground state obtained by RM1 semiempirical calculations with HyperChem 8.0 program. Color codes: CB7, green; SA^+, oxygen, red; nitrogen, blue; carbon, light blue.

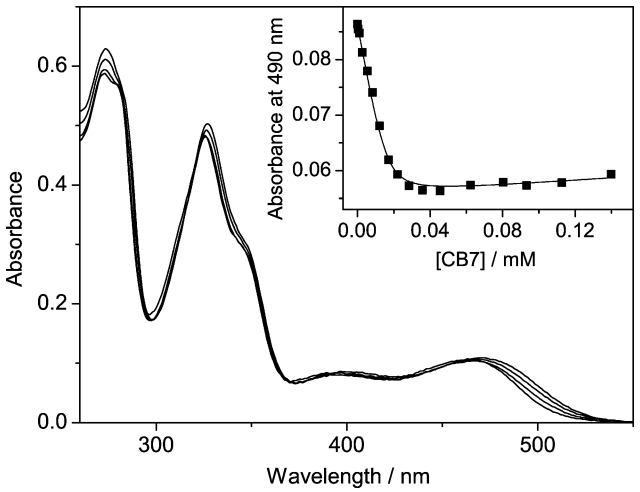

Fig. 5 Absorption spectrum of 16.4 μM sanguinarine at pH 4 in the presence of 0, 5.5, 12 and 140 μM CB7. Inset presents the absorbance change at 490 nm and the result of the nonlinear least-squares fit.

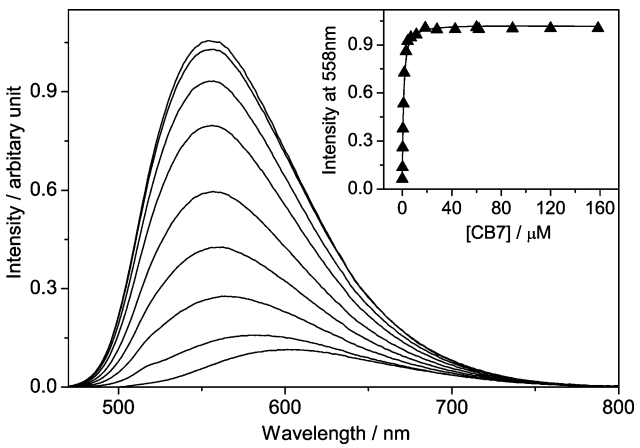

Fig. 6 Alteration of the fluorescence spectrum of 0.59 μM sanguinarine on addition of 0, 0.15, 0.35, 0.59, 0.96, 1.7, 3.1, 29 and 160 μM CB7 at pH 4. Inset displays the fluorescence intensity at 558 nm as a function of CB7 concentration. Excitation is at 440 nm. The line corresponds to the fitted function.

The open and filled squares in Fig. 7B show how the absorbance at 460 nm and the fluorescence intensity at 600 nm vary with increasing pH in the absence of CB7. The results of the two types of measurements (M) fit to the same trend. The Boltzmann function is widely used for the analysis of the sigmoid-shaped titration curves:[31]

$$M = \frac{M_0 - M_\infty}{1 + \exp[(pH - pK_a)/P]} + M_\infty \quad (3)$$

where P denotes a fitting parameter, pK_a represents the negative logarithm of the equilibrium constant $K_a = [SAOH][H^+]/[SA^+]$, M_0 and M_∞ are the absorbances or fluorescence intensities at low and high pH, respectively. The non-linear least-squares fit of eqn (3) to the experimental data gives $pK_a = 7.14 \pm 0.04$ in water. This result is in excellent agreement with that found by Absolínová and co-workers ($pK_a = 7.21 \pm 0.065$) in the solution of sanguinarine and 1 mM HNO_3.[25c]

As seen in Fig. 7B, the spectral changes occur at much higher pH in the presence of 0.1 mM CB7, when the most of SA^+ forms 1 : 1 inclusion complex. The pH dependence of the fluorescence intensity at 560 nm and the absorbance at 460 nm follow the same trend. A combined analysis of the two types of measurements gives $pK_a' = 10.83$ and the best fit of eqn (3) to the experimental data is plotted in Fig. 7B. The inclusion complex formation with CB7 leads to 3.69 pH unit displacement for the equilibrium between SA^+ and SAOH. Similar basicity enhancements promoted by CB7-confinement have been reported for amines, but in those cases, the effect originates from the preferential binding of the protonated guest.[7,22a,22b,32] The dissociation of the protonated amines is impeded by the stabilization of the N^+–H bond through hydrogen-bonding and ion–dipole interactions with the carbonyl groups on the CB[7] portal. The apparent pK_a enhancement upon the confinement of sanguinarine in CB7 is due to an entirely different effect. The macrocycle inhibits OH^- addition by protecting the position 6 of SA^+ against the nucleophilic attack. The NMR spectroscopic studies and quantum chemical

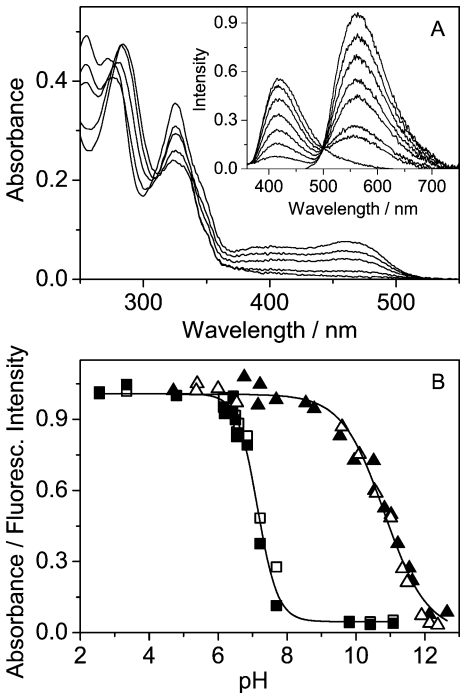

Fig. 7 (A) Absorption spectra of 16 μM sanguinarine in 100 μM CB7 solution at pH 7.16, 9.96, 10.83, 11.64 and 12.65. Inset shows the fluorescence spectrum of 1.9 μM sanguinarine in 653 μM CB7 solutions at pH 6.00, 9.60, 10.11, 10.59, 11.01, 11.36, 11.49 and 12.15. Excitation is at 309 nm. (B) Absorbance at 460 nm (■) and fluorescence intensity at 600 nm (□) for 10.5 μM sanguinarine aqueous solution as a function of pH. Absorbance of 16 μM sanguinarine at 460 nm in the presence of 100 μM CB7 (△) and fluorescence intensity of 1.9 μM sanguinarine at 560 nm (▲) in 653 μM CB7 solution at various pHs.

calculations demonstrated that position 6 is confined in the apolar CB7 cavity, but located around the plane of the oxygens of the macrocycle portal, whose high electron density hinders the approach of the OH^- anion to the carbon atom of the iminium bond of SA^+.

On the basis of the thermodynamic cycle in Scheme 3, the equilibrium constant of SAOH binding to CB7, $K_{SAOH} = [SAOH–CB7]/\{[SAOH][CB7]\}$ can be estimated from the measured $pK_a = 14 - pK_b$ and $pK_a' = 14 - pK_b'$ values and the equilibrium constant of SA^+–CB7 1 : 1 complex formation (K_1) using the following relationship:

$$K_{SAOH} = K_1 K_b/K_b' \quad (4)$$

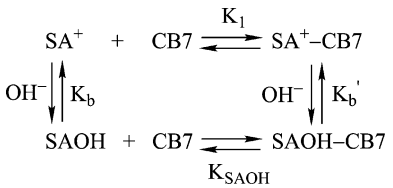

Scheme 3 Thermodynamic cycle of OH^- addition and 1 : 1 inclusion complex formation of sanguinarine.

From the pK_a and pK_a' values determined above, $K_b = 1.38 \times 10^{-7}$ M^{-1} and $K_b' = 6.76 \times 10^{-4}$ M^{-1} can be derived. The substitution of these values and $K_1 = 1.2 \times 10^6$ M^{-1}, the mean of the values derived form absorption and fluorescence titrations, into eqn (4) leads to $K_{SAOH} = 245$ M^{-1} as an estimate of the binding constant of SAOH–CB7 complex. This quantity cannot be determined directly by absorption or fluorescence measurements because the photochemical instability of SAOH (vide infra) is accompanied by a low solubility and small spectral changes upon confinement in CB7. The small binding affinity of SAOH to CB7 is not surprising because ion–dipole interactions cannot contribute to the driving force of complexation in the case of this neutral guest. Moreover, the addition of KOH brings about not only pH change but also leads to the coordination of K^+ to the carbonyl-fringed portals of CB7, hindering thereby the ingression of the organic guest.[33] Mezzini and co-workers reported 600 and 53 M^{-1} for the equilibrium constants of the first and second K^+ binding to CB7.[34] The competitive complexation of K^+ lessens the apparent binding constant of SAOH–CB7 formation. In the presence of 0.06 M KCl, which corresponds to the largest KOH concentration in the titration of CB7-bound sanguinarine, 3.9×10^4 M^{-1} was obtained for the apparent equilibrium constant of SA^+ inclusion in CB7. Although this is about 28-fold smaller than the value measured in neat water, it still ensures the complexation of about 96% of SA^+ at 653 μM CB7 concentration, which is employed in the fluorescence titration with KOH. Thus, we can conclude that the competitive binding of K^+ does not preclude SA^+–CB7 formation. At high pH, OH^- reacts probably with the small fraction of unbound SA^+, which shifts the complexation equilibrium toward dissociation. Taking the above estimated $K_{SAOH} = 245$ M^{-1} value, we can calculate that about 14% of SAOH is embedded in CB7 at the end of the fluorescence titration displayed in Fig. 7.

CB7-inhibited photooxidation

Maiti's group demonstrated that in the presence of oxygen SAOH undergoes an irreversible photooxidation in the excited singlet state producing 6-oxysanguinarine.[28] We studied the effect of CB7 on this reaction in 6.1 μM sanguinarine solution at pH 12.8 using excitation at 329 nm. The transformation of SAOH was followed by the detection of its fluorescence intensity at 480 nm. Fig. 8 shows that the gradual increase of CB7 concentration decreases the reaction conversion. This effect indicates that the encapsulated excited guest is protected against interaction with oxygen. Good linear correlations were obtained between the reciprocal fluorescence intensity and irradiation time (inset in Fig. 8) indicating that the disappearance of SAOH followed second order kinetics. From the slopes, 840, 400 and 270 $M^{-1}s^{-1}$ were derived for the apparent rate constant of SAOH decomposition in the presence of 0, 433 and 881 μM CB7. As photooxidation of SAOH is probably a multistep reaction, CB7 may also affect the rate constant of secondary reactions and the concentration of reactive intermediates. Considering the above estimated low fraction of the complexed SAOH under the experimental conditions of photoirradiation, the inhibition caused by CB7 is efficient since after 20 min reaction time, more than twice as large amount of SAOH remains unreacted in the presence of CB7 as in water. Unfortunately, the limited solubility of CB7 does not permit of the complete complexation of SAOH.

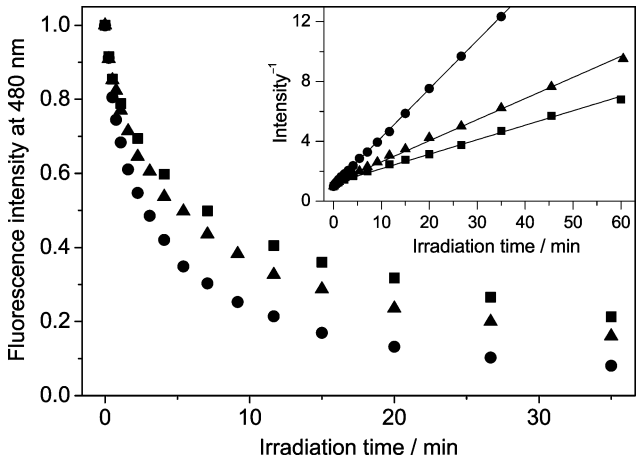

Fig. 8 Diminution of SAOH concentration with reaction time detected by the fluorescence intensity change upon irradiation at 329 nm. The initial solutions contain 6.1 μM sanguinarine, 0.06 M KOH and 0 (●), 0.43 (▲) or 0.81 mM (■) CB7. The inset shows that the photooxidation of SAOH follows second order kinetics with CB7 concentration dependent rate.

Conclusions

The iminium form of sanguinarine (SA^+) produces inclusion complex with not only one but also two CB7. In the stable 1 : 1 complex, the benzodioxole part of the isoquinoline moiety is encapsulated in the hydrophobic core of CB7, and the positive charge of the heterocyclic ring interacts with the oxygens of the macrocycle. Although the examined natural alkaloid can be embedded only partially in CB7, 1 : 1 complexation efficiently protects SA^+ against the nucleophilic attack at the 6 position. It also increases the photostability in alkaline solution and decelerates radiationless deactivation from the singlet-excited state. The more than 3 orders of magnitude difference between the equilibrium constants for the 1 : 1 CB7 complex formation of the two sanguinarine forms permits of the selective encapsulation of the biologically active SA^+. Therefore, inclusion complex formation with CB7 may be utilized not only for the stabilization of sanguinarine but also for drug delivery. The release of sanguinarine from the complex can be controlled by the change of pH.

Experimental

Sanguinarine chloride (Sigma) was used without further purification. The concentration of its solution was determined spectrophotometrically on the basis of the molar absorption coefficient (ε = 30700 M^{-1} cm^{-1} at 328 nm in acidic aqueous solution) reported in the literature.[24d,26] High purity cucurbit[7]uril, kindly provided by Dr Anthony I. Day, was dried in high vacuum for several days prior to use. The pH of the solutions, adjusted with HCl or KOH, was measured with a Consort C832 equipment. Glass electrode was calibrated at pH 4, 7 and 10 with buffer standards. The UV-visible absorption spectra were recorded on a Unicam UV 500 spectrophotometer. Corrected fluorescence spectra were obtained on a Jobin-Yvon Fluoromax-P photon-counting spectrofluorometer. Fluorescence decays were measured with time-correlated single-photon counting technique. A Picoquant diode laser (pulse duration *ca.* 70 ps, wavelength 372 nm) excited the samples, and the fluorescence decays were detected with a Hamamatsu R3809U-51 microchannel plate photomultiplier, which was connected to a Picoquant Timeharp 100 electronics (36 ps/channel time resolution). Time-resolved data were analyzed by a nonlinear least-squares reconvolution method using Picoquant FluoFit software. Molecular modeling calculations were carried out with RM1 method using HyperChem 8.0 program (Hypercube Inc., Gainesville, FL). NMR experiments were carried out on a Varian NMR System (600 MHz for ^1H) spectrometer. Samples were placed into 5 mm NMR tubes. ^1H chemical shifts were referenced to 7 volume% d_6-DMSO as internal standard (δ_{1H}^{DMSO} = 2.50 ppm). High purity deuterium oxide (99.9 atom%) solvent was purchased from Sigma-Aldrich Inc. Solvent suppression was performed by the standard PRESAT sequence. Spectra were processed by the spectrometer software package: VnmrJ 2.2C. Unless otherwise mentioned, NMR measurements were carried out at 283 K.

Acknowledgements

The authors very much appreciate the support of this work by the Hungarian Scientific Research Fund (OTKA, Grant K75015). The support of the Hungarian GVOP-3.2.1.-2004-04-0210/3.0 and KMOP-1.1.2-07/1-2008-0002 grants are gratefully acknowledged.

References

1 (*a*) K. H. Frömming and J. Szejtli, *Cyclodextrins in Pharmacy*, Kluwer Academic Publishers, Dordrecht, 1994; (*b*) M. E. Brewster and T. Loftsson, *Adv. Drug Delivery Rev.*, 2007, **59**, 645–666; (*c*) K. Uekama, F. Hirayama and T. Irie, *Chem. Rev.*, 1998, **98**, 2045–2076.
2 E. Da Silva, A. N. Lazar and A. W. Coleman, *J. Drug Del. Sci. Tech.*, 2004, **14**, 3–20.
3 F. Perret, A. N. Lazar and A. W. Coleman, *Chem. Commun.*, 2006, 2425–2438.
4 (*a*) J.-W. Lee, S. Samal, N. Selvapalam, H.-J. Kim and K. Kim, *Acc. Chem. Res.*, 2003, **36**, 621–630; (*b*) J. Lagona, P. Mukhopadhyay, S. Chakrabarti and L. Isaacs, *Angew. Chem., Int. Ed.*, 2005, **44**, 4844–4870; (*c*) K. Kim, *Chem. Soc. Rev.*, 2002, **31**, 96–107; (*d*) L. Isaacs, *Chem. Commun.*, 2009, 619–629.
5 (*a*) P. Montes-Navajas, M. González-Béjar, J. C. Scaiano and H. García, *Photochem. Photobiol. Sci.*, 2009, **8**, 1743–1747; (*b*) G. Hettiarachchi, D. Nguyen, J. Wu, D. Lucas, D. Ma, L. Isaacs and V. Briken, *PLoS One*, 2010, **5**, e10514; (*c*) V. D. Uzunova, C. Cullinane, K. Brix K, W. M. Nau and A. I. Day, *Org. Biomol. Chem.*, 2010, **8**, 2037–2042; (*d*) J. S. Liu and X. Z. Du, *J. Mater. Chem.*, 2010, **20**, 3642–3649; (*e*) F. J. McInnes, N. G. Anthony, A. R. Kennedy and N. J. Wheate, *Org. Biomol. Chem.*, 2010, **8**, 765–773.
6 N. Dong, S.-F. Xue, Q.-J. Zhu, Z. Tao, Y. Zhao and L.-X. Yang, *Supramol. Chem.*, 2008, **20**, 659–665.
7 R. Wang and D. H. Macartney, *Org. Biomol. Chem.*, 2008, **6**, 1955–1960.
8 I. W. Wyman and D. H. Macartney, *Org. Biomol. Chem.*, 2010, **8**, 247–252.
9 Y. J. Zhao, D. P. Buck, D. L. Morris, M. H. Pourgholami, A. I. Day and J. G. Collins, *Org. Biomol. Chem.*, 2008, **6**, 4509–4515.
10 Y. J. Zhao, M. H. Pourgholami, D. L. Morris, J. G. Collins and A. I. Day, *Org. Biomol. Chem.*, 2010, **8**, 3328–3337.
11 N. Saleh, A. L. Koner and W. M. Nau, *Angew. Chem., Int. Ed.*, 2008, **47**, 5398–5401.
12 (*a*) N. J. Wheate, A. I. Day, R. J. Blanch, A. P. Arnold, C. Cullinane and J. G. Collins, *Chem. Commun.*, 2004, 1424–1425; (*b*) Y. J. Jeon, S. Y. Kim, Y. H. Ko, S. Sakamoto, K. Yamaguchi and K. Kim, *Org. Biomol. Chem.*, 2005, **3**, 2122–2125; (*c*) N. J. Wheate, D. P. Buck, A. I. Day and J. G. Collins, *Dalton Trans.*, 2006, 451–458; (*d*) S. Kemp, N. J. Wheate, S. Wang, J. G. Collins, S. F. Ralph, A. I. Day, V. J. Higgins and J. P. Aldrich-Wright, *JBIC, J. Biol. Inorg. Chem.*, 2007, **12**, 969–979; (*e*) Y. J. Zhao, M. S. Bali, C. Cullinane, A. I. Day and J. G. Collins,

Dalton Trans., 2009, 5190–5198; (*f*) A. R. Kennedy, A. J. Florence, F. J. McInnes and N. J. Wheate, *Dalton Trans.*, 2009, 7695–7700.
13 D. P. Buck, P. M. Abeysinghe, C. Cullinane, A. I. Day, J. G. Collins and M. M. Harding, *Dalton Trans.*, 2008, 2328–2334.
14 E. Kim, D. Kim, H. Jung, J. Lee, S. Paul, N. Selvapalam, Y. Yang, N. Lim, C. G. Park and K. Kim, *Angew. Chem., Int. Ed.*, 2010, **49**, 4405–4408.
15 K. M. Park, D.-W. Lee, B. Sarkar, H. Jung, J. Kim, Y. H. Ko, K. E. Lee, H. Jeon and K. Kim, *Small*, 2010, **6**, 1430–1441.
16 C. R. Thomas, D. P. Ferris, J. H. Lee, E. Choi, M. H. Cho, E. S. Kim, J. F. Stoddart, J. S. Shin, J. Cheon and J. I. Zink, *J. Am. Chem. Soc.*, 2010, **132**, 10623–10625.
17 R. Wang, I. W. Wyman, S. Wang and D. H. Macartney, *J. Inclusion Phenom. Macrocyclic Chem.*, 2009, **64**, 233–237.
18 (*a*) M. Megyesi and L. Biczók, *J. Phys. Chem. B*, 2007, **111**, 5635–5639; (*b*) M. Megyesi and L. Biczók, *Chem. Phys. Lett.*, 2007, **447**, 247–251; (*c*) M. Megyesi and L. Biczók, *Chem. Phys. Lett.*, 2006, **424**, 71–76; (*d*) Z. Miskolczy and L. Biczók, *Chem. Phys. Lett.*, 2009, **477**, 80–84.
19 M. Megyesi, L. Biczók and I. Jablonkai, *J. Phys. Chem. C*, 2008, **112**, 3410–3416.
20 C.-F. Li, L.-M. Du, W.-Y. Wu and A.-Z. Sheng, *Talanta*, 2010, **80**, 1939–1944.
21 C.-F. Li, L.-M. Du and H.-M. Zhang, *Spectrochim. Acta, Part A*, 2010, **75**, 912–917.
22 (*a*) J. Mohanty, A. C. Bhasikuttan, W. M. Nau and H. Pal, *J. Phys. Chem. B*, 2006, **110**, 5132–5138; (*b*) M. Shaikh, J. Mohanty, P. K. Singh, W. M. Nau and H. Pal, *Photochem. Photobiol. Sci.*, 2008, **7**, 408–414; (*c*) A. Praetorius, D. M. Bailey, T. Schwarzlose and W. M. Nau, *Org. Lett.*, 2008, **10**, 4089–4092; (*d*) C. Klöck, R. N. Dsouza and W. M. Nau, *Org. Lett.*, 2009, **11**, 2595–2598; (*e*) M. Shaikh, S. D. Choudhury, J. Mohanty, A. C. Bhasikuttan, W. M. Nau and H. Pal, *Chem.–Eur. J.*, 2009, **15**, 12362–12370; (*f*) R. B. Wang, B. C. MacGillivray and D. H. Macartney, *Dalton Trans.*, 2009, 3584–3589.
23 (*a*) V. M. Adhami, M. H. Aziz, S. R. Reagan-Shaw, M. Nihal, H. Mukhtar and N. Ahmad, *Mol. Cancer Ther.*, 2004, **3**, 933–940; (*b*) N. Ahmad, S. Gupta, M. M. Husain, K. M. Heiskanen and H. Mukhtar, *Clin. Cancer Res.*, 2000, **6**, 1524–1528; (*c*) K. C. Godowski, *J. Clin. Dent.*, 1989, **1**, 96–101; (*d*) H. Liu, J. H. Wang, J. L. Zhao, S. Q. Lu, J. G. Wang, W. B. Jiang, Z. H. Ma and L. G. Zhou, *Nat. Prod. Commun.*, 2009, **4**, 1557–1560; (*e*) I. De Stefano, G. Raspaglio, G. F. Zannoni, D. Travaglia, M. G. Prisco, M. Mosca, C. Ferlini, G. Scambia and D. Gallo, *Biochem. Pharmacol.*, 2009, **78**, 1374–1381.
24 (*a*) J. Urbanová, P. Lubal, I. Slaninová, E. Táborská and P. Táborský, *Anal. Bioanal. Chem.*, 2009, **394**, 997–1002; (*b*) L.-P. Bai, Z. Cai, Z.-Z. Zhao, K. Nakatani and Z.-H. Jiang, *Anal. Bioanal. Chem.*, 2008, **392**, 709–716; (*c*) A. Sen and M. Maiti, *Biochem. Pharmacol.*, 1994, **48**, 2097–2102; (*d*) P. Giri and G. S. Kumar, *Biochim. Biophys. Acta, Gen. Subj.*, 2007, **1770**, 1419–1; (*e*) A Adhikari, M. Hossain, M. Maiti and G. S. Kumar, *J. Mol. Struct.*, 2008, **889**, 54–63.
25 (*a*) V. Simanek and V. Preinenger, *Heterocycles*, 1977, **6**, 475–497 ; (1977); (*b*) M. Maiti, R. Nandi and K. Chaudhuri, *Photochem. Photobiol.*, 1983, **38**, 245–249; (*c*) H. Absolínová, L. Jančář, I. Jančářová, J. Vičar and V. Kubáň, *Cent. Eur. J. Chem.*, 2009, **7**, 876–883.
26 R. R. Jones, R. J. Harkrader and G. L. Southard, *J. Nat. Prod.*, 1986, **49**, 1109–1111.
27 J. Dostál and M. Potáček, *Collect. Czech. Chem. Commun.*, 1990, **55**, 2840–2873.
28 G. S. Kumar, A. Das and M. Maiti, *J. Photochem. Photobiol., A*, 1997, **111**, 51–56.
29 M. Megyesi and L. Biczók, *J. Phys. Chem. B*, 2010, **114**, 2814–2819.
30 M. Janovská, M. Kubala, V. Simanek and J. Ulrichova, *Anal. Bioanal. Chem.*, 2009, **395**, 235–240.
31 C. Clower, K. M. Solntsev, J. Kowalik, L. M. Tolbert and D. Huppert, *J. Phys. Chem. A*, 2002, **106**, 3114–3122.
32 (*a*) H. Bakirci, A. L. Koner, T. Schwarzlose and W. M. Nau, *Chem.–Eur. J.*, 2006, **12**, 4799–4807; (*b*) R. Wang, L. Yuan and D. H. Macartney, *Chem. Commun.*, 2005, 5867–5869.
33 C. Márquez, R. R. Hudgins and W. M. Nau, *J. Am. Chem. Soc.*, 2004, **126**, 5806–5816.
34 E. Mezzini, F. Cruciani, G. F. Pedulli and M. Lucarini, *Chem.–Eur. J.*, 2007, **13**, 7223–7233.

